AIAA JOURNAL
Vol. 40, No. 7, July 2002

First-Order-Theory-Based Thermoelastic Stability of Functionally Graded Material Circular Plates

M. M. Najafizadeh*
Islamic Azad University, 14515-775 Tehran, Iran
and
M. R. Eslami†
Amirkabir University of Technology, 15914 Tehran, Iran

Thermal buckling of circular plates made of functionally graded material is discussed. The nonlinear equilibrium and linear stability equations are derived using variational formulations. The thermal buckling of solid circular plates under uniform temperature rise, gradient through the thickness, and linear temperature variation along the radius are considered, and the buckling temperatures are derived. The buckling temperatures are derived for simply supported and clamped edges. The results are verified with known results in the literature.

Nomenclature

a = radius of plate
E = Young's modulus
h = plate thickness
M_i = bending moment
M_i^T = thermal moment
N_i = in-plane force
N_i^T = thermal force
r = radial coordinate
u, w = radial and transverse displacements, respectively
z = axial coordinate
α_T = coefficient of thermal expansion
β_r = slope in radial direction
θ = circumferential coordinate

Introduction

IN recent years, functionally graded materials (FGMs) have gained considerable importance as materials to be used in extremely high-temperature environments such as the nuclear reactor and high-speed spacecraft industries.[1] FGMs are new materials, microscopically inhomogeneous, in which the mechanical properties vary smoothly and continuously from one surface to the other. This is achieved by gradually varying the volume fraction of the constituent materials. This continuous change in composition results in the graded properties of FGMs. These novel materials were first introduced in 1984 (Refs. 1 and 2). Typically, these materials are made from a mixture of ceramic and metal or from a combination of different metals. The advantage of using these materials is that they are able to withstand high-temperature gradient environments while maintaining their structural integrity. The ceramic constituent of the material provides the high-temperature resistance due to its low thermal conductivity. The ductile metal constituent, on the other hand, prevents fracture caused by stresses due to the high-temperature gradient in a very short period of time. Furthermore, a mixture of ceramic and metal with a continuously varying volume fraction can be easily manufactured.[2–6] This eliminates interface problems of composite materials, and thus, the stress distributions are smooth. FGMs were initially designed as thermal barrier materials for aerospace structural applications and fusion reactors. These materials are now developed for general use as structural elements in extremely high-temperature environments. A listing of different applications may be found in Ref. 7.

Circular plates loaded in compression are often employed as structural components in engineering systems. Several authors have investigated the elastic stability of composite circular plates subjected to various loadings and boundary conditions. Krizhevsky and Stavsky,[8] using Hamilton's variational principle, derived the equations of transversally isotropic, laminated, annular plates motion. Linearized vibration and buckling equations are obtained for the annular plates uniformly compressed in the radial direction. A closed form solution is given for the mode shapes in terms of the Bessel, power, and trigonometric functions. Thermoelastic buckling analysis of orthotropic solid circular plates based on first-order plate theory and the Sanders assumption is given by Najafizadeh and Eslami.[9]

Buckling analysis of FGM structures are rare in the literature. Birman[10] studied the buckling problem of a functionally graded composite rectangular plate subjected to the uniaxial compression. The stabilization of a functionally graded cylindrical shell under axial harmonic loading is investigated by Ng et al.[11] Javaheri and Eslami presented the thermal and mechanical buckling of rectangular FGM plates based on first- and higher-order plate theories.[12–15] The buckling analysis of circular FGM plates under radial compressive load is given by Najafizadeh and Eslami.[16]

The aim of the present paper is to derive the general thermoelastic equilibrium and stability equations for circular plates made of FGM from the energy method with the use of calculus of variations and compatible with the theory of buckling. Then, closed-form solutions for the circular plates subjected to thermal loads are obtained. The results are validated with the known data in the literature.

Analysis

Consider a circular plate of radius a and thickness h made of FGM, as shown in Fig. 1. The material properties of the FGM plate, such as the modulus of elasticity E and the coefficient of thermal expansion α, are assumed to be functions of the volume fraction of the constituent materials. When the coordinate axis across the plate thickness is denoted by z, as seen from Fig. 1, the functional relationships between E and α with z for a ceramic and metal FGM plate are assumed as[17]

$$E = E(z) = E_m + (E_c - E_m)[(2z + h)/2h]^k$$

$$\alpha = \alpha(z) = \alpha_m + (\alpha_c - \alpha_m)[(2z + h)/2h]^k, \qquad \nu = \nu_0 \quad (1)$$

where E_c, α_c, E_m, and α_m are the corresponding properties of the ceramic and metal, respectively, and k is the volume fraction exponent, which takes values greater than or equal to zero. The value of

Received 22 May 2001; revision received 8 January 2002; accepted for publication 22 January 2002.

*Ph.D. Student, Mechanical Engineering Department, Punak.
†Professor, Mechanical Engineering Department. Associate Fellow AIAA.

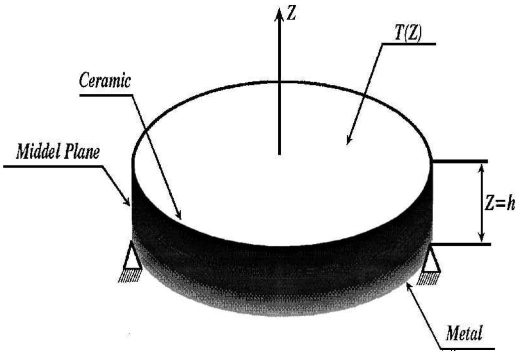

Fig. 1 Geometry of circular plate made of FGMs.

k equal to 0 represents a fully ceramic plate. The preceding power law assumption reflects a simple rule of mixtures used to obtain the effective properties of the ceramic–metal plate. The power law index k varies between 0 and infinity.[17] The rule of mixtures applies only to the thickness direction. The density of the plate varies according to the power law, and the power law exponent may be varied to obtain different distributions of the component materials through the thickness of the plate. Poisson's ratio ν is assumed to be constant across the plate thickness.

The two-dimensional stress–strain law for the plane-stress condition is given by

$$\epsilon_{rr} = [1/E(z)](\sigma_{rr} - \nu\sigma_{\theta\theta}) + \alpha(z)T$$

$$\epsilon_{\theta\theta} = [1/E(z)](\sigma_{\theta\theta} - \nu\sigma_{rr}) + \alpha(z)T, \qquad \epsilon_{r\theta} = [1/G(z)]\sigma_{r\theta} \tag{2}$$

The plate is assumed to be comparatively thin, and according to the Love–Kirchhoff assumptions, planes normal to the median surface are assumed to remain plane after deformation; thus, shear deformations normal to the plate are disregarded. Strain components at distance z from the middle plane are then given by

$$\epsilon_{rr} = \bar{\epsilon}_{rr} - zk_{rr}, \qquad \epsilon_{\theta\theta} = \bar{\epsilon}_{\theta\theta} - zk_{\theta\theta}, \qquad \epsilon_{r\theta} = \bar{\epsilon}_{r\theta} - 2zk_{r\theta} \tag{3}$$

where the z axis is measured across the plate thickness from the plate's middle plane. Here, $\bar{\epsilon}_{rr}$, $\bar{\epsilon}_{\theta\theta}$, and $\bar{\epsilon}_{r\theta}$ are the strain components in the median surface, and k_{rr}, $k_{\theta\theta}$, and $k_{r\theta}$ are the curvatures that can be expressed in term of the displacement components. The relations between the middle plane strains and the displacement components according to the Sanders assumption are (see Ref. 18)

$$\bar{\epsilon}_{rr} = \frac{\partial u}{\partial r} + \frac{1}{2}\left(\frac{\partial w}{\partial r}\right)^2, \qquad \bar{\epsilon}_{\theta\theta} = \frac{1}{r}\frac{\partial v}{\partial \theta} + \frac{u}{r} + \frac{1}{2}\left(\frac{1}{r}\frac{\partial w}{\partial \theta}\right)^2$$

$$\bar{\epsilon}_{r\theta} = \frac{1}{r}\frac{\partial u}{\partial \theta} + \frac{\partial v}{\partial r} - \frac{v}{r} + \left(\frac{1}{r}\frac{\partial w}{\partial r}\right)\frac{\partial w}{\partial \theta} \tag{4}$$

$$k_{rr} = -\frac{\partial^2 w}{\partial r^2}, \qquad k_{\theta\theta} = -\frac{1}{r}\frac{\partial w}{\partial r} - \frac{1}{r^2}\frac{\partial^2 w}{\partial \theta^2}$$

$$k_{r\theta} = \frac{-1}{r}\left(\frac{\partial^2 w}{\partial r \partial \theta}\right) + \frac{1}{r^2}\frac{\partial w}{\partial \theta} \tag{5}$$

When Eqs. (4) and (5) are substituted into Eqs. (3), the following expressions for the strain components are obtained:

$$\epsilon_{rr} = \frac{\partial u}{\partial r} + \frac{1}{2}\left(\frac{\partial w}{\partial r}\right)^2 - z\frac{\partial^2 w}{\partial r^2}$$

$$\epsilon_{\theta\theta} = \frac{1}{r}\frac{\partial v}{\partial \theta} + \frac{u}{r} + \frac{1}{2}\left(\frac{1}{r}\frac{\partial w}{\partial \theta}\right)^2 - z\left(\frac{1}{r}\frac{\partial w}{\partial r} + \frac{1}{r^2}\frac{\partial^2 w}{\partial \theta^2}\right)$$

$$\epsilon_{r\theta} = \frac{1}{r}\frac{\partial u}{\partial \theta} + \frac{\partial v}{\partial r} - \frac{v}{r} + \left(\frac{1}{r}\frac{\partial w}{\partial r}\right)\frac{\partial w}{\partial \theta}$$

$$+ 2z\left[\frac{-1}{r}\left(\frac{\partial^2 w}{\partial r \partial \theta}\right) + \frac{1}{r^2}\frac{\partial w}{\partial \theta}\right] \tag{6}$$

The total potential energy for the circular plate may be written as

$$V = \frac{1}{2}\int_0^r \int_0^{2\pi} \int_{-h/2}^{h/2} (\epsilon_{rr}\sigma_{rr} + \epsilon_{\theta\theta}\sigma_{\theta\theta} + \epsilon_{r\theta}\sigma_{r\theta}$$

$$- \alpha T\sigma_{rr} - \alpha T\sigma_{\theta\theta}) r \,\mathrm{d}r \,\mathrm{d}\theta \,\mathrm{d}z \tag{7}$$

On substitution of Eqs. (6) into Eq. (7) and integration with respect to z from $-h/2$ to $h/2$, the total potential energy is obtained as

$$V = \frac{A}{2(1-\nu^2)}\int_0^r \int_0^{2\pi}\left[\epsilon_{rr}^2 + \epsilon_{\theta\theta}^2 + 2\nu\epsilon_{rr}\epsilon_{\theta\theta} + \frac{1-\nu}{2}\epsilon_{r\theta}^2\right] r \,\mathrm{d}r \,\mathrm{d}\theta$$

$$+ \frac{B}{2(1-\nu^2)}\int_0^r \int_0^{2\pi}\Big[k_{rr}^2 + k_{\theta\theta}^2 + 2\nu k_{rr}k_{\theta\theta}$$

$$+ 2(1-\nu)k_{r\theta}^2\Big] r \,\mathrm{d}r \,\mathrm{d}\theta + \frac{2C}{(1-\nu^2)}\int_0^r \int_0^{2\pi}[\epsilon_{rr}k_{rr} + \epsilon_{\theta\theta}k_{\theta\theta}$$

$$+ \nu(\epsilon_{rr}k_{\theta\theta} + \epsilon_{\theta\theta}k_{rr}) + (1-\nu)\epsilon_{r\theta}k_{r\theta}] r \,\mathrm{d}r \,\mathrm{d}\theta - \frac{1}{1-\nu}$$

$$\times \int_0^r \int_0^{2\pi}\Big[(\epsilon_{rr} + \epsilon_{\theta\theta})T_m + (k_{rr} + k_{\theta\theta})T_b - T^*\Big] r \,\mathrm{d}r \,\mathrm{d}\theta \tag{8}$$

where

$$A = \int_{-h/2}^{h/2} E(z)\,\mathrm{d}z, \qquad B = \int_{-h/2}^{h/2} E(z)z^2\,\mathrm{d}z$$

$$C = \int_{-h/2}^{h/2} E(z)z\,\mathrm{d}z, \qquad T_m = \int_{-h/2}^{h/2} E(z)\alpha(z)T(z)\,\mathrm{d}z$$

$$T_b = \int_{-h/2}^{h/2} E(z)\alpha(z)T(z)z\,\mathrm{d}z, \qquad T^* = \int_{-h/2}^{h/2} E(z)\alpha^2(z)T^2(z)\,\mathrm{d}z \tag{9}$$

The equilibrium equations for circular plate made of the FGM using the Euler equations (see Ref. 18) are

$$N_{r,r} + \frac{1}{r}N_{r\theta,\theta} + \frac{N_r - N_\theta}{r} = 0, \qquad N_{r\theta,r} + \frac{1}{r}N_{\theta,\theta} + \frac{2}{r}N_{r\theta} = 0$$

$$\frac{\partial}{\partial\theta}\left(\frac{1}{r}N_\theta w_{,\theta} + N_{r\theta}w_{,r} + \frac{2}{r}M_{r\theta}\right) + \frac{\partial^2}{\partial r^2}(rM_r) + \frac{\partial}{\partial r}(rN_r w_{,r}$$

$$+ N_{r\theta}w_{,\theta} - M_\theta) + \frac{\partial^2}{\partial r\partial\theta}(2M_{r\theta}) + \frac{\partial^2}{\partial\theta^2}\left(\frac{1}{r}M_\theta\right) = 0 \tag{10}$$

where

$$N_r = [A/(1-\nu^2)][\epsilon_{rr} + \nu\epsilon_{\theta\theta}]$$

$$+ [C/(1-\nu^2)][k_{rr} + \nu k_{\theta\theta}] - T_m/(1-\nu)$$

$$N_\theta = [A/(1-\nu^2)][\epsilon_{\theta\theta} + \nu\epsilon_{rr}]$$

$$+ [C/(1-\nu^2)][k_{\theta\theta} + \nu k_{rr}] - T_m/(1-\nu)$$

$$N_{r\theta} = [A/2(1+\nu)]\epsilon_{r\theta} + [C/(1+\nu)]k_{r\theta}$$

$$M_r = [C/(1-\nu^2)][\epsilon_{rr} + \nu\epsilon_{\theta\theta}]$$

$$+ [B/(1-\nu^2)][k_{rr} + \nu k_{\theta\theta}] - T_b/(1-\nu)$$

$$M_\theta = [C/(1-\nu^2)][\epsilon_{\theta\theta} + \nu\epsilon_{rr}]$$

$$+ [B/(1-\nu^2)][k_{\theta\theta} + \nu k_{rr}] - T_b/(1-\nu)$$

$$M_{r\theta} = [C/2(1+\nu)]\epsilon_{r\theta} + [B/(1+\nu)]k_{r\theta} \tag{11}$$

Substitution from Eqs. (11) into the third of Eqs. (10), yields

$$N_{r,r}+\frac{1}{r}N_{r\theta,\theta}+\frac{N_r-N_\theta}{r}=0,\qquad N_{r\theta,r}+\frac{1}{r}N_{\theta,\theta}+\frac{2}{r}N_{r\theta}=0$$

$$\frac{B}{1-\nu^2}\nabla^4 w-N_r\frac{\partial^2 w}{\partial r^2}-\frac{1}{r}N_\theta\left(\frac{\partial w}{\partial r}+\frac{1}{r}\frac{\partial^2 w}{\partial \theta^2}\right)-2N_{r\theta}\left(\frac{-1}{r^2}\frac{\partial w}{\partial \theta}+\frac{1}{r}\frac{\partial^2 w}{\partial r\partial\theta}\right)+\frac{C}{1-\nu^2}\left(\frac{1-2\nu}{r^3}\frac{\partial v}{\partial\theta}-\frac{1-2\nu}{r^2}\frac{\partial^2 v}{\partial r\partial\theta}+\frac{1}{r^2}\frac{\partial u}{\partial r}-\frac{u}{r^3}-\frac{2}{r}\frac{\partial^2 u}{\partial r^2}-\frac{1}{r^3}\frac{\partial^2 u}{\partial\theta^2}-\frac{1}{r^3}\frac{\partial^2 u}{\partial\theta^2}-\frac{1}{r^2}\frac{\partial^3 u}{\partial^2\theta\partial r}-\frac{1}{r}\frac{\partial^3 v}{\partial^2 r\partial\theta}-\frac{1}{r^3}\frac{\partial^3 v}{\partial\theta}-\frac{\partial^3 u}{\partial r^3}\right)=0 \tag{12}$$

The stability equations are derived using the variational method. If V is the total potential energy of the plate, the expansion of V about the equilibrium state into the Taylor series yields

$$\Delta V=\delta V+\tfrac{1}{2}\delta^2 V+\tfrac{1}{6}\delta^3 V+\cdots \tag{13}$$

The stability of the plate in the neighborhood of the equilibrium condition may be determined by the sign of the second variation of V. The condition $\delta^2 V=0$ is used to derive the stability equations for buckling problems.[18]

Let us assume that u_i^* denotes the displacement component of the equilibrium state and δu_i^* the virtual displacement corresponding to a neighboring state. When the variation with respect to u_i^* is denoted by $\bar{\delta}$, the following rule, known as the Trefftz rule, is stated for the determination of the lowest critical load.[18] The external load acting on the original configuration is considered to be the critical buckling load if the following variational equation is satisfied:

$$\bar{\delta}(\delta^2 V)=0 \tag{14}$$

This rule provides the governing equations that determine the lowest critical loads. The state of stable equilibrium of a general circular plate under thermal load may be designated by u_0, v_0, and w_0. The displacement components of the neighboring state are

$$u=u_0+u_1,\qquad v=v_0+v_1,\qquad w=w_0+w_1 \tag{15}$$

where u_1, v_1, and w_1 are arbitrary small increments of displacements. Substituting Eqs. (15) in Eq. (8) and collecting the second-order terms, we obtain the second variation of the potential energy, which when applying the Euler equations, results in the stability equations as

$$N_{r_1,r}+\frac{1}{r}N_{r\theta_1,\theta}+\frac{N_{r_1}-N_{\theta_1}}{r}=0$$

$$N_{r\theta_1,r}+\frac{1}{r}N_{\theta_1,\theta}+\frac{2}{r}N_{r\theta_1}=0$$

$$\frac{B}{1-\nu^2}\nabla^4 w_1-N_{r_0}\frac{\partial^2 w_1}{\partial r^2}-\frac{1}{r}N_{\theta_0}\left(\frac{\partial w_1}{\partial r}+\frac{1}{r}\frac{\partial^2 w_1}{\partial\theta^2}\right)-2N_{r\theta_0}\left(\frac{-1}{r^2}\frac{\partial w_1}{\partial\theta}+\frac{1}{r}\frac{\partial^2 w_1}{\partial r\partial\theta}\right)+\frac{C}{1-\nu^2}\left(\frac{1-2\nu}{r^3}\frac{\partial v_1}{\partial\theta}-\frac{1-2\nu}{r^2}\frac{\partial^2 v_1}{\partial r\partial\theta}+\frac{1}{r^2}\frac{\partial u_1}{\partial r}-\frac{u_1}{r^3}-\frac{2}{r}\frac{\partial^2 u}{\partial r^2}-\frac{1}{r^3}\frac{\partial^2 u_1}{\partial\theta^2}-\frac{1}{r^3}\frac{\partial^2 u_1}{\partial\theta^2}-\frac{1}{r^2}\frac{\partial^3 u_1}{\partial^2\theta\partial r}-\frac{1}{r}\frac{\partial^3 v_1}{\partial^2 r\partial\theta}-\frac{1}{r^3}\frac{\partial^3 v_1}{\partial\theta}-\frac{\partial^3 u_1}{\partial r^3}\right)=0 \tag{16}$$

where

$$N_{r_1}=\frac{A}{1-\nu^2}\left[\frac{\partial u_1}{\partial r}+\nu\left(\frac{1}{r}\frac{\partial v_1}{\partial\theta}+\frac{u_1}{r}\right)\right]+\frac{C}{1-\nu^2}\left[-\frac{\partial^2 w_1}{\partial r^2}-\frac{\nu}{r}\frac{\partial w_1}{\partial r}-\frac{\nu}{r^2}\frac{\partial^2 w_1}{\partial\theta^2}\right]$$

$$N_{\theta_1}=\frac{A}{1-\nu^2}\left[\frac{u_1}{r}+\frac{1}{r}\frac{\partial v_1}{\partial\theta}+\nu\frac{\partial u_1}{\partial r}\right]+\frac{C}{1-\nu^2}\left[-\frac{1}{r}\frac{\partial w_1}{\partial r}-\frac{1}{r^2}\frac{\partial w_1}{\partial\theta^2}-\nu\frac{\partial^2 w_1}{\partial r^2}\right]$$

$$N_{r\theta_1}=A\left[\frac{1}{r}\frac{\partial u_1}{\partial\theta}+\frac{\partial v_1}{\partial r}-\frac{v_1}{r}\right]+C\left[-\frac{1}{r}\frac{\partial^2 w_1}{\partial\theta\partial r}+\frac{1}{r^2}\frac{\partial w_1}{\partial\theta}\right]$$

$$N_{r_0}=\frac{A}{1-\nu^2}\left[\frac{\partial u_0}{\partial r}+\nu\left(\frac{1}{r}\frac{\partial v_0}{\partial\theta}+\frac{u_0}{r}\right)\right]+\frac{C}{1-\nu^2}\left[-\frac{\partial^2 w_0}{\partial r^2}-\frac{\nu}{r}\frac{\partial w_0}{\partial r}-\frac{\nu}{r^2}\frac{\partial^2 w_0}{\partial\theta^2}\right]-\frac{T_m}{1-\nu}$$

$$N_{\theta_0}=\frac{A}{1-\nu^2}\left[\frac{u_0}{r}+\frac{1}{r}\frac{\partial v_0}{\partial\theta}+\nu\frac{\partial u_0}{\partial r}\right]+\frac{C}{1-\nu^2}\left[-\frac{1}{r}\frac{\partial w_0}{\partial r}-\frac{1}{r^2}\frac{\partial^2 w_0}{\partial\theta^2}-\nu\frac{\partial^2 w_0}{\partial r^2}\right]-\frac{T_m}{1-\nu}$$

$$N_{r\theta_0}=A\left[\frac{1}{r}\frac{\partial u_0}{\partial\theta}+\frac{\partial v_0}{\partial r}-\frac{v_0}{r}\right]+C\left[-\frac{1}{r}\frac{\partial^2 w_0}{\partial r\partial\theta}+\frac{1}{r^2}\frac{\partial w_0}{\partial\theta}\right]$$

$$M_{r_1}=\frac{C}{1-\nu^2}\left[\frac{\partial u_1}{\partial r}+\nu\left(\frac{u_1}{r}+\frac{1}{r}\frac{\partial v_1}{\partial\theta}\right)\right]+\frac{B}{1-\nu^2}\left[-\frac{\partial^2 w_1}{\partial r^2}-\nu\left(\frac{1}{r}\frac{\partial w_1}{\partial r}+\frac{1}{r^2}\frac{\partial^2 w_1}{\partial\theta^2}\right)\right]$$

$$M_{\theta_1}=\frac{C}{1-\nu^2}\left[\frac{1}{r}\frac{\partial v_1}{\partial\theta}+\frac{u_1}{r}+\nu\frac{\partial u_1}{\partial r}\right]+\frac{B}{1-\nu^2}\left[-\frac{1}{r}\frac{\partial w_1}{\partial r}-\frac{1}{r^2}\frac{\partial^2 w_1}{\partial\theta^2}-\nu\frac{\partial^2 w_1}{\partial r^2}\right]$$

$$M_{r\theta_1}=C\left[\frac{1}{r}\frac{\partial u_1}{\partial\theta}+\frac{\partial v_1}{\partial r}-\frac{v_1}{r}\right]+B\left[\frac{1}{r^2}\frac{\partial w_1}{\partial\theta}-\frac{1}{r}\frac{\partial^2 w_1}{\partial r\partial\theta}\right] \tag{17}$$

Thermal Buckling Analysis

Let us consider a circular plate, in the absence of mechanical loading, subjected to a thermal field $T=T(r,z)$. We also limit the discussion to the case of polar symmetry. With this condition, the first and third of stability equations (16), using Eqs. (17), become

$$\frac{B}{1-\nu^2}\nabla^4 w_1-N_{r_0}\frac{\mathrm{d}^2 w_1}{\mathrm{d}r^2}-\frac{1}{r}N_{\theta_0}\left(\frac{\mathrm{d}w_1}{\mathrm{d}r}\right)+\frac{C}{1-\nu^2}\left(\frac{1}{r^2}\frac{\mathrm{d}u_1}{\mathrm{d}r}-\frac{u_1}{r^3}-\frac{2}{r}\frac{\mathrm{d}^2 u_1}{\mathrm{d}r^2}-\frac{\mathrm{d}^3 u_1}{\mathrm{d}r^3}\right)=0$$

$$\frac{A}{1-\nu^2}\left(\frac{\mathrm{d}^2 u_1}{\mathrm{d}r^2}+\frac{1}{r}\frac{\mathrm{d}u_1}{\mathrm{d}r}-\frac{u_1}{r^2}\right)+\frac{C}{1-\nu^2}\left(-\frac{\mathrm{d}^3 w_1}{\mathrm{d}r^3}-\frac{1}{r}\frac{\mathrm{d}^2 w_1}{\mathrm{d}r^2}+\frac{1}{r^2}\frac{\mathrm{d}w_1}{\mathrm{d}r}\right)=0 \tag{18}$$

In Eqs. (18), N_{r0} and $N_{\theta 0}$ are the prebuckling thermal forces that must be calculated. From the first of Eqs. (12), we have

$$N_{\theta 0}=rN_{r_0,r}+N_{r_0} \tag{19}$$

Substituting Eq. (19) into the first of Eqs. (18), we find

$$B'\nabla^4 w_1-\frac{1}{r}\frac{\mathrm{d}}{\mathrm{d}r}\left(rN_{r_0}\frac{\mathrm{d}w_1}{\mathrm{d}r}\right)+C'\left(\frac{1}{r^2}\frac{\mathrm{d}u_1}{\mathrm{d}r}-\frac{u_1}{r^3}-\frac{2}{r}\frac{\mathrm{d}^2 u_1}{\mathrm{d}r^2}-\frac{\mathrm{d}^3 u_1}{\mathrm{d}r^3}\right)=0 \tag{20}$$

where

$$B' = B/(1-\nu^2), \qquad C' = C/(1-\nu^2) \tag{21}$$

The prebuckling force-displacement relations from Eq. (17) based on the membrane plate theory are[18]

$$N_{r_0} = \frac{A}{1-\nu^2}\left[\frac{\mathrm{d}u_0}{\mathrm{d}r} + \nu\frac{u_0}{r}\right] - \frac{T_m}{1-\nu}$$

$$N_{\theta_0} = \frac{A}{1-\nu^2}\left[\frac{u_0}{r} + \nu\frac{\mathrm{d}u_0}{\mathrm{d}r}\right] + \frac{T_m}{1-\nu} \tag{22}$$

Substituting Eqs. (22) into the first of the equilibrium equations (12) yields

$$\frac{A}{1-\nu^2}\left[r\frac{\mathrm{d}^2u_0}{\mathrm{d}r^2} + \frac{\mathrm{d}u_0}{\mathrm{d}r} - \frac{u_0}{r}\right] - \frac{T_{m,r}}{1-\nu} = 0 \tag{23}$$

When the temperature is a function of thickness of the plate, or in the case of uniform temperature rise, we have

$$T_{m,r} = 0 \tag{24}$$

Substituting into Eq. (23) gives

$$\frac{\mathrm{d}^2u_0}{\mathrm{d}r^2} + \frac{1}{r}\frac{\mathrm{d}u_0}{\mathrm{d}r} - \frac{u_0}{r^2} = 0 \tag{25}$$

Solution of Eq. (25) is

$$u_0 = c_1 r + c_2(1/r) \tag{26}$$

When a solid circular plate is considered with the following boundary conditions:

$$u_0 = \text{finite} \quad \text{at} \quad r = 0, \qquad u_0 = 0 \quad \text{at} \quad r = a \tag{27}$$

the constants of integration $c_1 = c_2 = 0$, and from Eq. (26),

$$u_0 = 0 \tag{28}$$

Therefore, from Eqs. (22) we have

$$N_{r0} = N_{\theta_0} = -T_m/(1-\nu) = -N^T_{r0} \tag{29}$$

Thus, for solution of the stability equation, the following set of coupled stability equations must be considered:

$$A'\left(\frac{\mathrm{d}^2u_1}{\mathrm{d}r^2} + \frac{1}{r}\frac{\mathrm{d}u_1}{\mathrm{d}r} - \frac{u_1}{r^2}\right) + C'\left(-\frac{\mathrm{d}^3w_1}{\mathrm{d}r^3} - \frac{1}{r}\frac{\mathrm{d}^2w_1}{\mathrm{d}r^2} + \frac{1}{r^2}\frac{\mathrm{d}w_1}{\mathrm{d}r}\right) = 0$$

$$B'\nabla^4 w_1 - \frac{1}{r}\frac{\mathrm{d}}{\mathrm{d}r}\left(rN_{r_0}\frac{\mathrm{d}w_1}{\mathrm{d}r}\right) + C'\left(\frac{1}{r^2}\frac{\mathrm{d}u_1}{\mathrm{d}r} - \frac{u_1}{r^3} - \frac{2}{r}\frac{\mathrm{d}^2u_1}{\mathrm{d}r^2} - \frac{\mathrm{d}^3u_1}{\mathrm{d}r^3}\right) = 0 \tag{30}$$

where

$$A' = A/(1-\nu^2), \qquad B' = B/(1-\nu^2)$$

$$C' = C/(1-\nu^2) \tag{31}$$

Calling

$$\frac{\mathrm{d}w_1}{\mathrm{d}r} = Y, \qquad \frac{\mathrm{d}^2w_1}{\mathrm{d}r^2} = \frac{\mathrm{d}Y}{\mathrm{d}r}, \qquad \frac{\mathrm{d}^3w_1}{\mathrm{d}r^3} = \frac{\mathrm{d}^2Y}{\mathrm{d}r^2} \tag{32}$$

and substituting Eq. (32) into the first of stability Eq. (30), we find

$$r^2q'' + rq' - q = 0 \tag{33}$$

where

$$q = A'u_1 - C'Y \tag{34}$$

Solution of Eq. (33) gives

$$q = c_3 r + c_4\left(\frac{1}{r}\right) = A'u_1 - C'\frac{\mathrm{d}w_1}{\mathrm{d}r} \tag{35}$$

with boundary conditions

$$u_1 = \frac{\mathrm{d}w_1}{\mathrm{d}r} = \text{finite} \quad \text{at} \quad r = 0$$

$$u_1 = \frac{\mathrm{d}w_1}{\mathrm{d}r} = 0 \quad \text{at} \quad r = a \tag{36}$$

Applying the boundary conditions yields

$$c_3 = 0, \qquad c_4 = 0 \tag{37}$$

Substituting Eq. (37) into Eq. (35) gives

$$q = 0 \tag{38}$$

and from Eq. (34), we have

$$u_1 = \frac{C'}{A'}\frac{\mathrm{d}w_1}{\mathrm{d}r} \tag{39}$$

Substituting Eq. (39) into the second of stability equations (30) gives

$$D_1\nabla^4 w_1 = \frac{1}{r}\frac{\mathrm{d}}{\mathrm{d}r}\left(rN_{r0}\frac{\mathrm{d}w_1}{\mathrm{d}r}\right) \tag{40}$$

where

$$D_1 = B' - P, \qquad P = C'^2/A' \tag{41}$$

From Eq. (29) we have

$$N_{r0} = -N^T_{r0} \tag{42}$$

Substituting Eq. (42) into Eq. (40) and with one-step integration with respect to r, we get

$$r^2\beta'' + r\beta' + \beta(\lambda^2r^2 - 1) = 0 \tag{43}$$

where

$$\beta = -\frac{\mathrm{d}w_1}{\mathrm{d}r}, \qquad \lambda^2 = \frac{N^T_{r0}}{D_1} \tag{44}$$

The solution of Eq. (43) is

$$\beta = c_5 J_1(\lambda r) + c_6 Y_1(\lambda r) \tag{45}$$

where J_1 and Y_1 are the Bessel functions of first order and first and second kinds, respectively, and c_5 and c_6 are integration constants. However, $\beta = 0$ at $r = 0$, and $Y_1(0) \to \infty$. Therefore, $c_6 = 0$ and

$$\beta = c_5 J_1(\lambda r) \tag{46}$$

For the clamped edge, $\beta = 0$ at $r = a$, where a is the plate radius. Therefore,

$$J_1(x) = 0, \qquad x = \lambda a \tag{47}$$

and the lowest critical thermal load is expressed in terms of $x_1 = \lambda_1 a$, the first zero of the Bessel function of first kind and order one, as

$$\lambda a = 3.831 \tag{48}$$

Using the value of λa and substituting into Eqs. (44) gives

$$N^T_{r0} = 14.68\left(D_1/a^2\right) \tag{49}$$

From Eq. (29) for the case of uniform temperature rise, the thermal buckling load of the clamped circular plate reduces to

$$T_{m_{cr}} = 14.68(1-\nu)\left(D_1/a^2\right) \tag{50}$$

For the case of simply supported plate, we similarly obtain

$$T_{m_{cr}} = 4.2(1-\nu)\left(D_1/a^2\right) \tag{51}$$

To calculate the critical buckling temperature for the case of gradient through the thickness temperature, the one-dimensional equation of heat conduction in the z direction must be solved. The equation for the temperature through the thickness is as follows:

$$-\frac{\mathrm{d}}{\mathrm{d}z}\left[k(z)\frac{\mathrm{d}T}{\mathrm{d}z}\right] = 0 \tag{52}$$

with boundary conditions

$$T = T_c$$

at $z = h/2$ and

$$T = T_m \tag{53}$$

at $z = -h/2$. This equation yields the temperature distribution through the thickness of the plate for different values of the volume fraction index k. For the case of $k = 2$, the general solution of Eq. (52) satisfying the the boundary conditions (53) is

$$T(z) = 0.461\Delta T \tanh^{-1}\left[0.974\left(z/h + \tfrac{1}{2}\right)\right] + T_m \tag{54}$$

where $\Delta T = T_c - T_m$ is the difference of the temperature between $z = -h/2$ and $h/2$. When this temperature distribution is applied gradually, the resulting buckling loads for clamped edge circular plate is

$$T_{m_{cr}} = 29.28(1-\nu)\left(D_1'/a^2\right) \tag{55}$$

where, at $k = 2$,

$$D_1' = D_1 \tag{56}$$

For a simply supported circular plate, the thermal buckling load is

$$T_{m_{cr}} = 8.4(1-\nu)\left(D_1'/a^2\right) \tag{57}$$

For the case of linear temperature variation along the direction of the radius, such that

$$T = (\Delta T/a)r + T_0 \tag{58}$$

where $\Delta T = T_a - T_0$, the critical thermal buckling load for the clamped circular plate with the assumption that $T_0 = 0$ is

$$T_{m_{cr}} = 19.87(1-\nu)\left(D_1/a^2\right) \tag{59}$$

Results and Discussion

Axisymmetric stability and thermal buckling equations of a circular plate subjected to uniform temperature rise, gradient through the thickness, and linear temperature variation along the radius were derived in the preceding section. These types of thermal bucklings are frequently needed in the design stage of circular plates. Thermal buckling loads are summarized in Table 1, which were obtained by the use of Eqs. (31) and (41).

To illustrate the behavior of the derived buckling equations, an FGM plate of aluminum and alumina is considered. The Young's modulus, Poisson's ratio, density, conductivity, and coefficient of thermal expansion for aluminum are 70 GPa, 0.3, 2707 kg/m^3, 204 W/mK, and 23.0×10^{-6}(1/°C). For alumina, they are 380 GPa, 0.3, 3800 kg/m^3, 10.4 W/mK, and 7.4×10^{-6} (1/°C), respectively. Note that Poisson's ratio is selected to be constant and equal to 0.3.

Figures 2 and 3 show the buckling temperature T_{cr} vs the ratio of thickness to radius h/a for the case of uniform temperature rise with the simply supported and clamped supported edges for various values of the volume fraction exponent k. The value of the exponent k is varied between 0 and 0.5, where 0 indicates a full ceramic plate and 0.5 indicates an FGM plate. It is seen that the buckling temperature of the full ceramic plate is higher than the FGM plate. That is, the thermal instability of FGM plate is lower than full ceramic plate. Figure 4 shows the buckling temperature T_{cr} vs the ratio of thickness to radius h/a for the case of linear temperature variation along the plate radius with the clamped support edges for various values of the volume fraction exponent k. For this case, it is observed that, as the values of k are decreased, the buckling temperatures are increased.

Figure 5 shows the variation of the temperature through the thickness of the aluminum–alumina plates for various values of the volume fraction exponent k. The temperature distribution was obtained by solving the one-dimensional heat conduction equation through

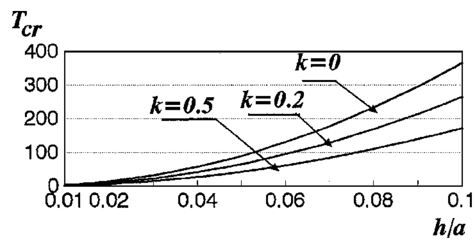

Fig. 2 Buckling temperature vs ratio *h/a* for simply supported plate and uniform temperature rise.

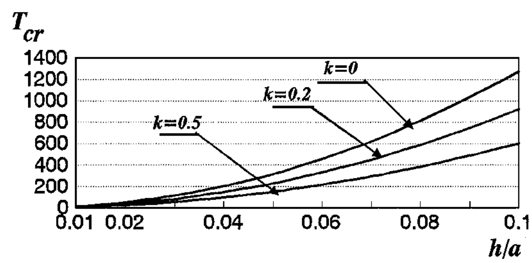

Fig. 3 Buckling temperature vs ratio *h/a* for clamped plate and uniform temperature rise.

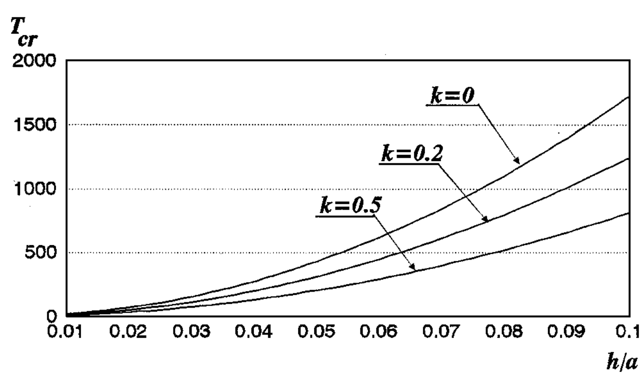

Fig. 4 Buckling temperature vs ratio *h/a* for clamped plate and linear temperature along the radius.

Table 1 Thermal buckling of circular FGM plate

Type of load	Simply supported	Clamped
Uniform temperature rise	$T_{m_{cr}} = [4.2/(1+\nu)][(AB-C^2)/Aa^2]$	$T_{m_{cr}} = [14.68/(1+\nu)][(AB-C^2)/Aa^2]$
Gradient through the thickness	$T_{m_{cr}} = [8.4/(1+\nu)][(AB-C^2)/Aa^2]$	$T_{m_{cr}} = [29.28/(1+\nu)][(AB-C^2)/Aa^2]$
Gradient through the radius	——	$T_{m_{cr}} = [19.87/(1+\nu)][(AB-C^2)/Aa^2]$

Table 2 Thermal buckling of circular isotropic plate

Type of load	Simply supported	Clamped
Uniform temperature rise	$T_{m\text{cr}} = [4.2/12(1+\nu)](h/a)^2(1/\alpha_c)$	$T_{m\text{cr}} = [14.68/12(1+\nu)](h/a)^2(1/\alpha_c)$
Gradient through the thickness	$T_{m\text{cr}} = [8.4/12(1+\nu)](h/a)^2(1/\alpha_c)$	$T_{m\text{cr}} = [29.28/12(1+\nu)](h/a)^2(1/\alpha_c)$
Gradient through the radius	—	$T_{m\text{cr}} = [19.87/12(1+\nu)](h/a)^2(1/\alpha_c)$

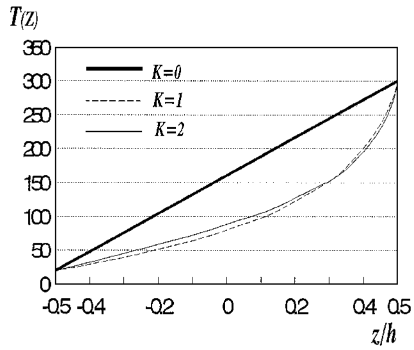

Fig. 5 Temperature distribution vs ratio *z/h* for gradient temperature through the thickness of the plate.

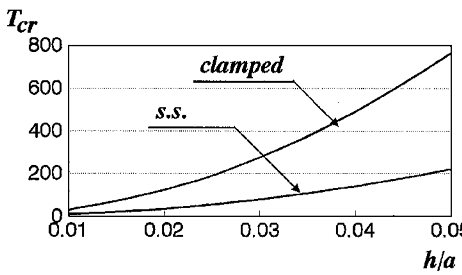

Fig. 6 Buckling temperature vs ratio *h/a* for gradient through the thickness temperature and *k* = 2.

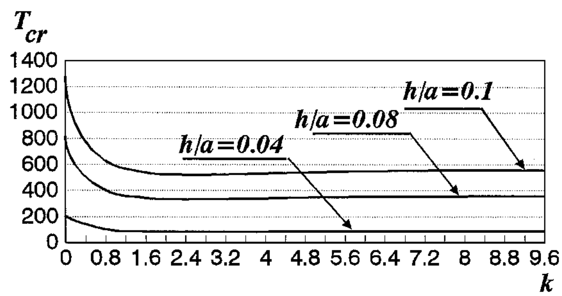

Fig. 7 Buckling temperature vs volume fraction exponent *k* for clamped plate and uniform temperature rise and for *h/a* = 0.04, 0.08, and 0.1.

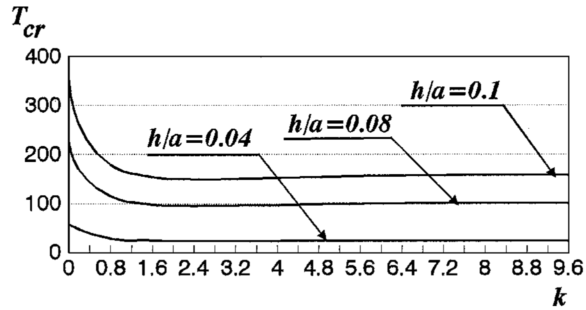

Fig. 8 Buckling temperature vs volume fraction exponent *k* for simply supported plate and uniform temperature rise and for *h/a* = 0.04, 0.08, and 0.1.

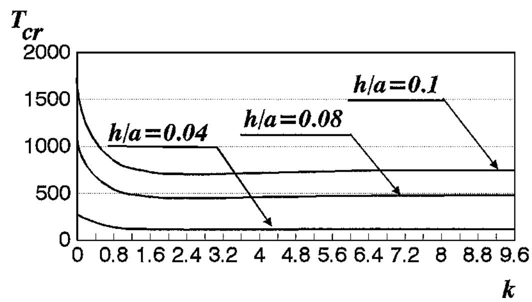

Fig. 9 Buckling temperature vs volume fraction exponent *k* for clamped plate and linear temperature along the radius and for *h/a* = 0.04, 0.08, and 0.1.

the thickness, by assuming that the conductivity varies according to Eq. (1). The conduction equation was solved by imposing the temperature boundary conditions at the top and bottom surfaces of the plate. The result of the analysis is plotted in Fig. 5. As the thermal boundary condition, the temperatures of the top ceramic surface was assumed to be 300°C, and the lower metallic surface was assumed to be 20°C (Ref. 17). It is assumed that, at any value of the thickness coordinate, the temperature is the same at all points in the plane. Figure 5 shows that the temperature distribution in the FGM plates ($k = 1$ and 2) across the thickness, for fixed surface boundary temperatures, are below that of a fully ceramic plate ($k = 0$).

Figure 6 shows the buckling temperature T_{cr} vs the ratio of thickness to radius h/a for the case of gradient through the thickness temperature, with the simply supported and clamped edges for value of the volume fraction exponent $k = 2$. In Fig. 6, the buckling temperature increases as h/a increases. Also, the clamped boundary condition provides a more stable plate configuration.

Figures 7–9 represent the buckling temperature T_{cr} vs volume fraction exponent k for $h/a = 0.04$, 0.08, and 0.1. The value of the exponent k is varied between 0 and 10. It is seen that the buckling temperature for the isotropic material, where $k = 0$, is higher than the FGM plate. Also, as h/a is increased, the buckling temperature is increased, as expected.

To prove the validity of the present formulations, results were obtained for isotropic plates and compared with existing references in the literature. For isotropic circular plate, from Eq. 9, we have

$$C = \int_{-h/2}^{h/2} E(z) z \, \mathrm{d}z = 0, \qquad B = \frac{E_c h^3}{12} \tag{60}$$

Then, from Eqs. (9) and Table 1, we find the buckling formula for the isotropic solid circular plates as given in Table 2.

The results shown in Table 2 were previously obtained by Najafizadeh and Eslami.[9] Note that for homogeneous isotropic circular plates the critical temperature is independent of Young's modulus. For the FGM plates, the buckling temperature is directly related to the modulus of elasticity E_c and E_m, in addition to its dependency on the coefficient of thermal expansion α_c and α_m.

Conclusions

Circular plates are widely used in structural design problems. When such a member is subjected to a thermal environment, its thermal buckling capacity is important in the design stage. For a design engineer, the closed-form solution for the buckling temperature of such a member is essential because the design may be quickly checked. In this paper, the closed-form solution for the buckling temperature of solid circular plates under commonly practiced temperature distribution in design are given. More complicated temperature distribution in design may be expected in circular plates under working conditions, but the related buckling temperature may then be obtained through numerical methods. The aim of this paper has been to avoid such complicated analysis and, rather, to provide simple closed-form solutions for commonly practiced circular plate design problems. In conclusion, FGMs may present an attractive tool for a designer. These materials can be optimized to reduce the cost and weight of structures and to tailor their properties according to design requirements. Note that the thermal buckling capacity of the FGM plates is, in general, lower than those of the isotropic ceramic plates with the similar geometries.

References

[1]Yamanouchi, M., and Koizumi, M., "Functionally Gradient Materials," *Proceedings of the First International Symposium on Functionally Graded Materials*, Functionally Graded Materials Forum, Sendai, Japan, 1990, pp. 327–332.

[2]Koizumi, M., "The Concept of FGM," *Ceramic Transactions, Functionally Gradient Materials*, Vol. 34, 1993, pp. 3–10.

[3]Sata, N., "Characteristic of SiC-TiB2 Composites as the Surface Layer of SiC–TiB2–Cu Functionally Gradient Materials Produced by Self-Propagating High-Temperature Synthesis," *Ceramic Transactions, Functionally Gradient Materials*, Vol. 34, 1993, pp. 109–116.

[4]Yamaoka, H., and Yaki, M., "Fabrication of Functionally Gradient Materials by Slurry Stacking and Sintering Process," *Ceramic Transactions, Functionally Gradient Materials*, Vol. 34, 1993, pp. 165–172.

[5]Rabin, B. H., and Heaps, R. J., "Powder Processing of Ni-Al2O3 FGM," *Ceramic Transactions, Functionally Gradient Materials*, Vol. 34, 1993, pp. 173–180.

[6]Fukui, Y., "Fundamental Investigation of Functionally Gradient Materials Manufacturing System Using Centrifugal Force," *International Journal of the Japan Society of Mechanical Engineering*, Vol. 4, No. 1, 1991, pp. 144–148.

[7]*Survey for Application of FGM*, FGM Forum, Japan Society of Non-Traditional Technology, Dept. of Material Science and Engineering, Tsinghua Univ., Tokyo, 1991.

[8]Krizhevsky, G., and Stavsky, Y., "Refined Theory for Vibrations and Buckling of Laminated Isotropic Annular Plates," *International Journal of Mechanical Science*, Vol. 38, No. 5, 1996, pp. 539–555.

[9]Najafizadeh, M. M., and Eslami, M. R., "Thermoelastic Stability of Orthotropic Circular Plates," *Journal of Thermal Stresses* (to be published).

[10]Birman, V., "Buckling of Functionally Graded Hybrid Composite Plates," *Proceeding of the 10th Conference on Engineering Mechanics*, Vol. 2, 1995, pp. 1199–1202.

[11]Ng, T. Y., Lam, Y. K., Liew, K. M., and Reddy, J. N., "Dynamic Stability Analysis of Functionally Graded Cylindrical Shell under Periodic Axial Loading," *International Journal of Solids and Structures*, Vol. 38, 2001, pp. 1295–1300.

[12]Javaheri, R., and Eslami, M. R., "Thermal Buckling of Functionally Graded Plates," *AIAA Journal*, Vol. 40, No. 1, 2002, pp. 162–169.

[13]Javaheri, R., and Eslami, M. R., "Buckling of Functionally Graded Plates Under In-Plane Compressive Loading," *ZAMM*, Vol. 82, No. 4, 2002, pp. 277–283.

[14]Javaheri, R., and Eslami, M. R., "Mechanical Buckling of Functionally Graded Plates Based on Higher Order Theory," *Journal of Strain Analysis* (submitted for publication).

[15]Javaheri, R., and Eslami, M. R., "Thermal Buckling of Functionally Graded Plates Based on Higher Order Theory," *Journal of Thermal Stresses* (to be published).

[16]Najafizadeh, M. M., and Eslami, M. R., "Thermoelastic Stability of Circular Plates Composed of Functionally Graded Materials Based on First Order Theory," *International Journal of Mechanical Sciences* (submitted for publication).

[17]Reddy, J. N., and Praveen, G. N., "Nonlinear Transient Thermoelastic Analysis of Functionally Graded Ceramic-Metal Plates," *International Journal of Solids and Structures*, Vol. 33, No. 33, 1998, pp. 4457–4476.

[18]Brush, D. O., and Almorth, B. O., *Buckling of Bars, Plates and Shells*, McGraw–Hill, New York, 1975, p. 79.

A. N. Palazotto
Associate Editor